

FRACTURE OF ASPHALT

by

JOHN STANLEY MARSH
B.S.C.E., University of Kentucky
(1963)

Submitted in partial fulfillment
of the requirements for the degree of
Master of Science in Civil Engineering

at the
Massachusetts Institute of Technology

(1966)

Signature of Author
Department of Civil Engineering, August 23, 1966

Certified by
Thesis Supervisor

Accepted by
Chairman, Departmental Committee on Graduate Students

ABSTRACT

FRACTURE OF ASPHALT

by

JOHN STANLEY MARSH

Submitted to the Department of Civil Engineering on August 23, 1966, in partial fulfillment of the requirements for the degree of Master of Science in Civil Engineering.

The Griffith theory of brittle fracture and its application to the fracture of asphalt are discussed. The critical strain-energy release rate is determined for three asphalts at different degrees of aging, loading rates, and thermal conditions. The results of this study indicate that the asphalts do behave as brittle, amorphous materials at low temperatures and that the critical strain-energy release rate can be used to study this behaviour.

Thesis Supervisor:

F. Moavenzadeh

Title:

Associate Professor

ACKNOWLEDGMENTS

I wish to express my sincere appreciation to Dr. F. Moavenzadeh, whose advice, direction, and encouragement were very helpful in the completion of this thesis. In addition, through our association, he has been a source of inspiration.

My deepest gratitude goes to the Goodyear Fellowship Program of the Goodyear Tire and Rubber Company whose monetary support has made this thesis possible.

I wish to acknowledge Mr. Arthur Rudolph for his invaluable supervision in the manufacture of much of the equipment used in this study.

Final thanks are due my wife and my parents for their patience, understanding, and constant support.

TABLE OF CONTENTS

	<u>PAGE</u>
I. Title Page	1
II. Abstract	2
III. Acknowledgments.	3
IV. Table of Contents	4
V. Body of text	6
Introduction	6
Review of Literature	7
The Griffith Theory of Brittle Fracture	7
Modifications of Griffith's Theory.	9
Applications of Brittle Failure Theory to Asphalt	10
Method of Determining the Critical Strain-Energy Release Rate	11
Objectives and Scope	14
Materials	15
Procedure	18
Specimen Preparation	18
Aging of the Asphalt	19
Testing	19
Results and Discussion of Results	20
Effect of Depth of Notch	21
Effect of Rate of Loading	21
Effect of Temperature	28
Effect of Different Asphalts	28
Effect of Aging	33

TABLE OF CONTENTS (Continued)

	<u>PAGE</u>
Conclusions	37
VI. References	38
VII. Appendices	39
Definitions of Symbols	40
List of Figures	41
List of Tables	43

INTRODUCTION

The failure of paving asphalt mixtures is in general divided into three categories (1)*: instability, disintegration, and fracture or cracking. Some of the factors included in disintegration, such as low tensile strength and brittleness of the binder, are also, at least indirectly, related to the cracking phenomena. Cracking of the asphaltic mixtures is considered to be primarily due to shrinkage, brittleness, and slippage of the asphalt binder. The quality and quantity of the asphaltic binder and the change in its characteristics over its service life are, therefore, found to have significant influence on the cracking of the pavements. Finn (2), however, points out that as yet there has been no consideration of the fracture strength of asphalt binder in the asphalt paving mix design requirements.

Asphalt becomes a brittle, glassy material at low temperatures, and this is primarily when cracks are developed in the asphaltic mixture. Cracking generally occurs either in the asphalt or at the interface of asphalt and aggregates. It, therefore, seems that the fracture and factors affecting the fracture of asphalt, could be analyzed using the theory of brittle fracture developed for amorphous materials. This analysis would be most helpful in explaining the cracking or fracture failure of paving asphalt mixtures.

*Numbers in parenthesis refer to References.

REVIEW OF LITERATURE

This section reviews briefly the theory of brittle fracture, modifications of Griffith's theory, and the application of this theory to asphaltic materials.

The Griffith Theory of Brittle Fracture

The theory of brittle failure has been developed in an attempt to better understand and explain the phenomenon of the fracture of certain materials, in a brittle fashion, at stresses far below their theoretical atomic bond strengths. The basic concept behind the theory of brittle failure, as presented by Griffith (3), was that, since the material failed when the average strain energy was far below the theoretical value required for failure, the strain energy was nonuniformly distributed. This nonuniform distribution of strain energy was attributed to the presence of small inherent cracks which acted as stress concentrators and thereby produced the corresponding concentrations of strain energy.

Inglis (4), for an infinite plate of unit thickness containing a very flat, elliptical hole with a major axis of length c perpendicular to a stress field, σ , applied at the edges of the plate, determined that the maximum tensile stress would occur at the ends of the major axis, and it is equal to:

$$\sigma_m = 2\sigma (c/\rho)^{1/2} \quad (1)$$

where σ_m is the maximum tensile stress which occurs, in the vicinity of the crack, and ρ is the radius of curvature at the ends of the major axis of the hole, or crack. If it is assumed that the material would fail

for some critical value of σ_m , then as ρ approached zero, the value of σ required to cause failure would also approach zero. This, however, is not the case; for, even with the sharpest cracks, there is still an appreciable value of tensile strength present upon failure.

The presence of tensile strength when the crack tip radius approaches zero was explained by Griffith (5) using the concept of surface energy and the principle of the conservation of energy. It was shown that, for the case of plane stress, the excess strain energy of the plate described by Inglis over that of a plate without a crack would be

$$U = \frac{\pi c^2 \sigma^2}{E} \quad (2)$$

per unit thickness of the plate. The work done in creating new surface energy as the crack extends is given as

$$W = 4\gamma'c \quad (3)$$

per unit thickness of the plate where γ' is the surface energy of the material per unit area. The factor of four is present due to the fact that two surfaces are being created at each end of the crack as the crack propagates.

Equating the change in the strain energy to the change in the work done for an infinitesimal increase of c , gives

$$\sigma = \sqrt{\frac{2\gamma'E}{\pi c}} \quad (4)$$

which is the well-known Griffith formula. For the case of plane ^{stress}, E must be replaced by $E/(1-\mu^2)$ and Equation 4 becomes

$$\sigma = \sqrt{\frac{2\gamma'E}{\pi(1-\mu^2)c}} \quad (5)$$

where μ is Poisson's ratio of the material. For the cases where the crack is an ellipsoid, and where the crack edges approach each other tangentially at each end, it has been shown that Equations 4 and 5 hold with minor variations in the numerical factors.

Verification of this work by Griffith has been given by several investigators including Griffith (3) and others as discussed by Orowan (6), for various materials. They have confirmed that the presence of very small cracks greatly reduce the measured tensile strengths of materials which fail in a brittle fashion. Furthermore, it was found (6) that surface cracks are usually most critical in the process of brittle failure.

Modifications of Griffith's Theory

For materials in which plastic flow is present before the onset of brittle failure, it has been suggested, by Irwin (7) and Orowan (8), that Griffith's formula, in a modified form, can be used as long as the plastic strains tended to occur only in regions close to the boundaries of the crack. In this case, the term for surface energy in Equations 4 and 5 must be replaced by a term that includes the work of the plastic strains as well as the work of creating new surface energy. Therefore, Equation 4 becomes

$$\sigma = \sqrt{\frac{2 \gamma_p E}{\pi c}} \quad (6)$$

where γ_p is the sum of all the work done in propagating the crack. γ_p is called the surface work term. This modified form of Griffith's formula has been applied to a wide range of materials, such as plastics and metals, which exhibit behaviour as described, i.e., plastic strains which, occur-

ring close to the crack boundaries, precede brittle failure. These studies have been successful on the most part.

Another modification to Griffith's work is the suggestion, by Irwin (9), that the strain-energy release rate, which can be determined by taking the derivative of Equation 2 to give

$$G = \frac{2\pi c \sigma^2}{E} \quad (7)$$

for the case of plane stress, is the important factor, or the true driving force, in crack propagation. The value of the strain-energy release rate at the onset of rapid crack propagation has been designated as the critical strain-energy release rate, G_c . It has been suggested (10) that, since different loading conditions could produce the same stress concentration at the tip of the crack, this critical value of the strain-energy release rate would be a constant for the material much as the modulus of elasticity is a constant for the material.

Applications of Brittle Failure Theory to Asphalt

Asphalt is a visco-elastic material whose properties are dependent on the shear rate and temperature, as well as the degree to which it has been aged. It is known that, at extreme low temperatures, the asphalt shows almost complete brittle behaviour. It would be expected, however, that at normal service temperatures, it would show a certain degree of plastic flow, which depends upon the temperature, the rate of loading, and the degree of aging. Due to this plastic flow, it is difficult to interpret the surface fracture work term since it could not be determined how much of the energy was consumed by plastic flow and how much was due

to the surface energy.

It would seem more reasonable, therefore, to determine the critical strain-energy release rate for the asphalt subjected to different conditions of temperature, rate of loading, and degree of aging. If the critical strain-energy release rate is a true property of the material, then some knowledge about the brittle behaviour of asphalt should be gained by applying the modified Griffith theory to fracture phenomena of the asphalt. The critical strain-energy release rate would be expected to be dependent on the parameters of temperature, rate of loading, and degree of aging much as would the modulus of elasticity of a material be dependent on these parameters.

Method of Determining the Critical Strain-Energy Release Rate

Two methods have been developed, as discussed by Kaplan (11), for the determination of the critical strain-energy release rate, both of which employ notched beam specimens tested in bending. One of these methods, the so-called direct experimental method, which was not used in this study, requires the calculation of the change in the spring constant as a function of the crack length. Preliminary investigation showed that this calculation was highly inaccurate, at best, when applied to asphalt. This could possibly be attributed to the presence of plastic flow, in varying quantities, in the specimens. Therefore, the second method, namely the analytical method, was used for determining the critical strain-energy release rate in this study.

Due to the fact that notched beams will be used, the expression for the strain-energy release rate, Equation 7, will require some modification.

Since this type of test employs a surface notch, there will be only one point of stress concentration, and therefore, the right-hand side of Equation 7 must be divided by a factor of two. Also, E must be replaced by $E/(1-\mu^2)$ since the dimensions of the test specimens will be such that this will be a case of plane strain. These modifications give

$$G = \frac{\pi(1-\mu^2)c\sigma^2}{E} \quad (8)$$

as the expression for the strain-energy release rate. For the case of rectangular beams, Equation 8 has been written in the form

$$G = \frac{(1-\mu^2)\sigma_n^2 h}{E} f(c/d) \quad (9)$$

where σ_n is the nominal bending stress at the root of the notch, $f(c/d)$ is a function of the notch depth ratio, as shown in Figure 1, and h is the depth of the unnotched portion of the beam. Equation 9 is the expression used in the analytical method to determine the strain-energy release rate.

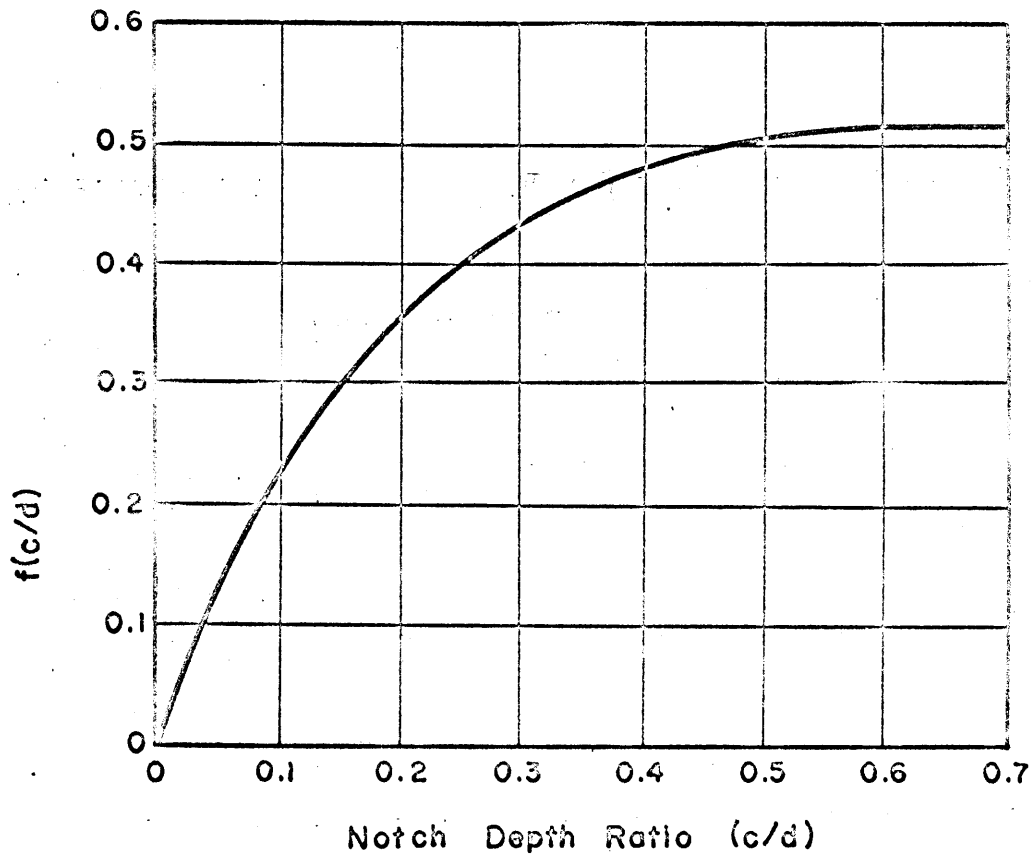


Figure 1 -- Values of $f(c/d)$ versus the Notch Depth Ratio

OBJECTIVES AND SCOPE

The objective of this study is to establish the applicability of the Griffith theory of brittle fracture to the fracture of asphalt and thus to gain some fundamental knowledge of the fracture phenomena of asphalt. To accomplish this objective, three asphalts of different rheological properties were chosen and tested under different loading and thermal conditions. The variables included three temperatures, three rates of loading, and three degrees of aging of the asphalt, as given in Table 1. One of the asphalts was tested under almost all possible combinations of the variables while the other two asphalts were tested under representative combinations of the variables in order to determine comparative behaviour of the different asphalts.

Table 1

Test Variables Used in this Study

Temperature	-7°F.	0°F.	+7°F.
Loading Rate (in/min.)	0.05	0.10	0.20
Hours of Aging at 375°F.	0	3	6

MATERIALS

The three asphalts used in this study were a 60-70 penetration grade asphalt cement from a Venezuelan crude, an AC-20 grade asphalt cement coded B-3056, and an AC-20 grade asphalt cement coded B-2960. The latter two were used in the "Asphalt Institute-Bureau of Public Roads" cooperative work. Table 2 shows the results of conventional tests on each of these asphalts.

Figure 2 is a plot of data showing the shear rate versus shear stress for the three asphalts at a test temperature of 25° Centigrade (12). This log-log representation results in a straight line and can be represented by

$$\tau = A (\dot{\gamma})^n \quad (10)$$

where A and n are constants which vary with the test temperature. The slope of the lines in Figure 2 is the inverse of n, and would be unity for a perfectly Newtonian material. As its value decreased from unity, the non-Newtonian behaviour increased. Therefore, the relative Newtonian response of the three asphalts can be determined from this plot. The 60-70 penetration grade asphalt is the most Newtonian of the three while the one coded B-3056 is the least Newtonian. Moavenzadeh and Stander (12) point out that the value of n decreases with decreasing temperature which indicates a more non-Newtonian response at lower temperatures. It is also indicated (12) that, for the three asphalts, the psuedo-plastic behaviour increases with decreasing temperature and increases with increasing aging.

Table 2

Results of Conventional Tests on Asphalts Used in this Study

Test	Asphalt		
	60-70	B-3056	B-2960
Specific Gravity	1.010	1.020	1.034
Softening Point, Ring and Ball	123°F.	---	125°F.
Ductility 77°F.	150+cm	250+cm	---
Penetration 100 gm, 5 sec, 77° F. 200 gm, 60 sec, 39.4° F.	63 23.5	--- 30	--- ---
Flash Point, Cleveland Open Cup	455°F.	545°F.	515°F.

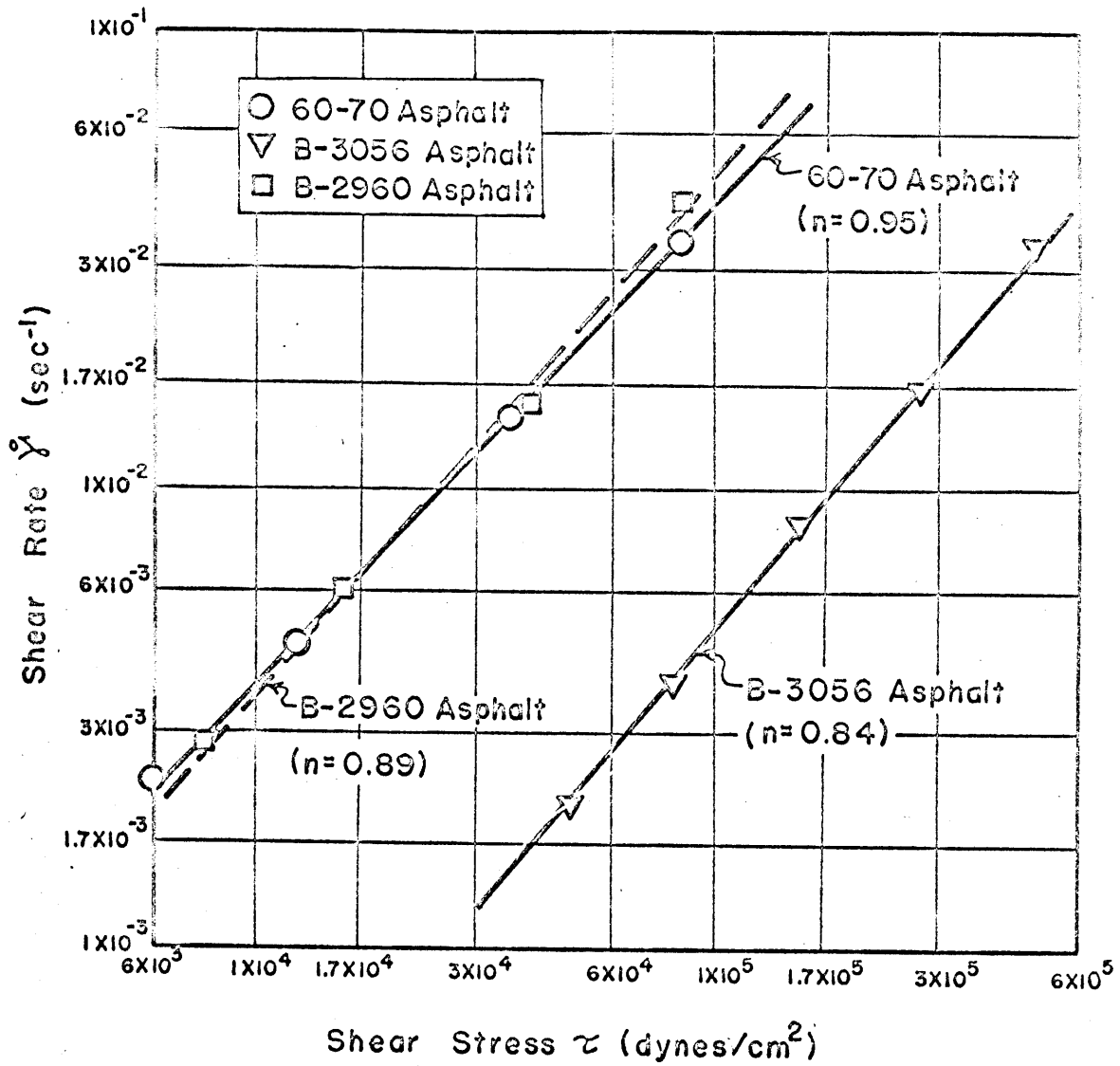


Figure 2 -- Shear Rate versus Shear Stress at 25°C.

PROCEDURE

Specimen Preparation

The basic specimen shape used was a notched, five inch long beam with a cross section measuring one-half inch by one-half inch. Figure 3 shows the notch geometry and the three point bending method of loading apparatus. Three depths of notch, one-sixteenth, one-eighth, and three-sixteenths of an inch, were used. These were made by using different inserts in the mold which gave the depth and the shape of notch desired.

To make the specimens, the mold and asphalt were heated to 125° Centigrade. The mold was overfilled slightly to allow for a decrease in volume as the asphalt cooled. After the cooling to room temperature, the mold was placed in a refrigerator and cooled to 15° Fahrenheit. Before the beams were removed from the mold, the excess asphalt was removed using a warm spatula. The prepared beams were stored in an airtight, water-free plexiglass box until testing.

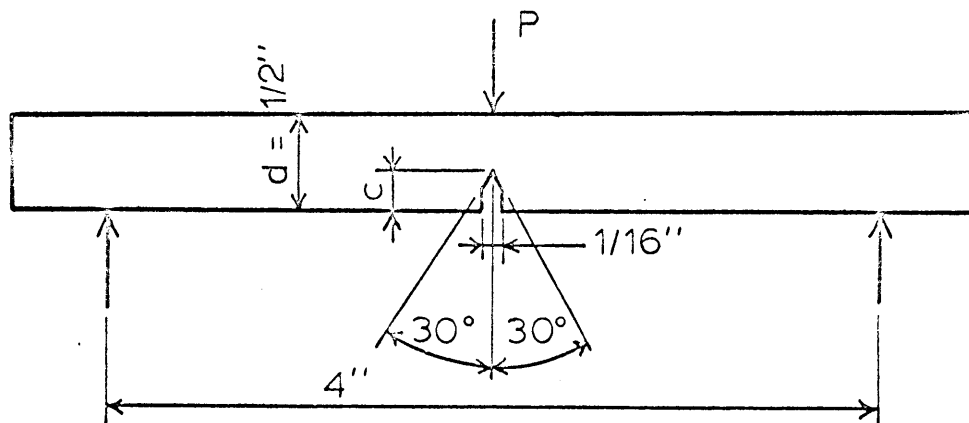


Figure 3 -- Notch Geometry and Method of Loading of the Beams

Aging of the Asphalt

Aging of the asphalts was accomplished by filling pyrex glass, petri dishes, approximately one-eighth of an inch deep, and heating them in a forced air oven at 375° for either three hours or six hours. After aging, the asphalts were poured into pint cans, covered immediately, and stored until needed.

Testing

The bending test was done in an Instron Testing Machine using a silicone oil, constant temperature bath in which the temperature was controlled to $\pm 0.2^{\circ}$ F. A pre-cooled specimen was placed in the loading frame and the crosshead of the Instron was started. Loading rates of 0.05, 0.10 and 0.20 inches per minute were used. Data output consisted of a plot of load versus time.

RESULTS AND DISCUSSION OF RESULTS

In this section, the results of mid-span bending tests on asphaltic beams are presented and discussed. In all cases, the failure of the beams was catastrophic, i.e., the load increased continuously with a constant rate until failure. A schematic diagram of the load-deflection curve is shown in Figure 4.

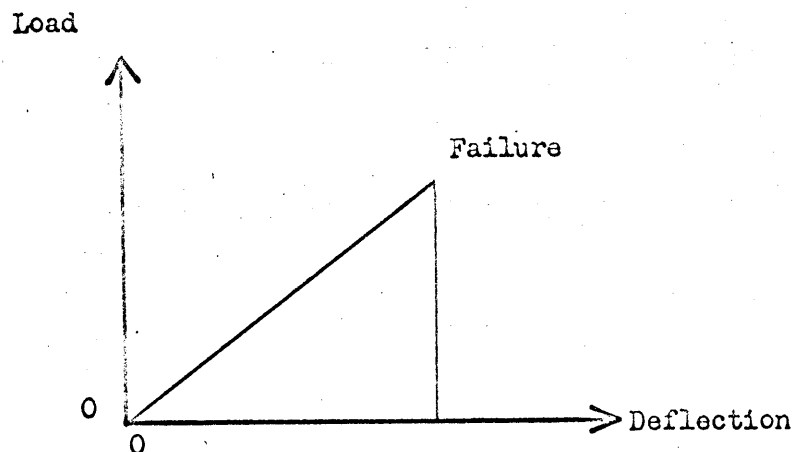


Figure 4 -- Schematic Load-Deflection Diagram

The appearance of the fracture surface, for all beams, was a smooth, glassy surface indicating a brittle failure. For some beams, there were "river" markings adjacent to the notch covering approximately five to ten per cent of the unnotched portion of the beam. No regularity was noticed to be associated with the appearance of these markings.

The modulus of elasticity, for each set of test conditions, was determined using the slopes of the load-deflection curves of unnotched beams and the standard deflection formula for a three point bending test, which

is

$$y = \frac{l}{48} \cdot \frac{P l^3}{E I} \quad (11)$$

where y is the maximum deflection of the beam, l is the span length, P is the applied load, and I is the moment of inertia of the beam. The average modulus of elasticity for each test condition is given in Table 3. It can be seen from this table that, for increasing rate of loading or decreasing temperature, the modulus of elasticity increases, which is the expected behaviour for asphalts. Poisson's ratio was assumed to be one-half in all cases. Table 4 gives the values of $f(c/d)$ for each corresponding notch depth ratio. These were determined from Figure 1.

Effect of Depth of Notch

The variations of the critical strain-energy release rate versus the notch depth ratio, as calculated from the analytical method, are given in Table 5 for each set of test conditions. The results shown are the averages of two, and sometimes three, tests on different specimens. Table 6 gives the averages of these values over each set of notch depth ratios and Table 7 gives the coefficient of variation for each set. The mean of the coefficients of variation is 4.0 per cent which is good agreement for the overall work and indicates that G_c is a true property of the material, in this case, asphalt.

Effect of Rate of Loading

In Figures 5 through 7, the values of G_c are plotted versus the notch depth ratio for unaged 60-70 penetration grade asphalt, for three different

Table 3
Calculated Moduli of Elasticity* (psi)

Asphalt	Aging at 375°F.	Rate of Deflection (in/min)	Test Temperature		
			+7°F.	0°F.	-7°F.
60-70	0	.05	19,900	67,600	90,000
		.10	53,100	71,600	98,900
		.20	54,600	73,000	99,200
	3 Hrs.	.10		74,200	
	6 Hrs.	.10		63,200	
B-2960	0	.10	16,700	30,600	
	6 Hrs.	.10		38,300	
B-3056	0	.10	81,000	95,100	
	6 Hrs.	.10		104,100	

* - Determined using the three point bending deflection formula.

Table 4
Values of f(c/d) Used

c/d	f(c/d)
0.125	0.28
0.250	0.40
0.375	0.47

Table 5

Values of the Critical Strain-Energy Release Rate (in-lb/in²)
for Different Notch Depth Ratios

Asphalt	Aging at 375°F.	Rate of Deflection (in/min)	Notch Depth Ratio	Test Temperature		
				+7°F.	0°F.	-7°F.
60-70	0	.05	.125	.0169	.0145	.0268
			.250	.0178	.0139	.0250
			.375	.0173	.0148	.0266
		.10	.125	.0190	.0182	.0158
			.250	.0188	.0185	.0173
			.375	.0184	.0183	.0165
		.20	.125	.0283	.0202	.0310
			.250	.0268	.0184	.0284
			.375	.0275	.0192	.0293
	3 Hrs.	.10	.125		.0265	
			.250		.0265	
			.375		.0229	
6 Hrs.	.10	.125		.0288		
		.250		.0260		
		.375		.0300		
B-2960	0	.10	.125	.0516	.0231	
			.250	.0511	.0242	
			.375	.0517	.0234	
	6 Hrs.	.10	.125		.0539	
			.250		.0583	
			.375		.0521	
B-3056	0	.10	.125	.0248	.0172	
			.250	.0246	.0195	
			.375	.0222	.0195	
	6 Hrs.	.10	.125		.0154	
			.250		.0149	
			.375		.0153	

Table 6

Average Values of the Critical Strain-Energy
Release Rate (in-lb/in²)

Asphalt	Aging at 375°F.	Rate of Deflection (in/min)	Test Temperature		
			+7°F.	0°F.	-7°F.
60-70	0	.05	.0173	.0114	.0264
		.10	.0187	.0183	.0165
		.20	.0275	.0189	.0296
	3 Hrs.	.10		.0253	
	6 Hrs.	.10		.0283	
B-2960	0	.10	.0515	.0234	
	6 Hrs.	.10		.0548	
B-3056	0	.10	.0239	.0187	
	6 Hrs.	.10		.0152	

Table 7

Values of the Coefficient of Variation* (per cent)

Asphalt	Aging at 375°F.	Rate of Deflection (in/min)	Test Temperature		
			+7°F.	0°F.	-7°F.
60-70	0	.05	2.5	3.2	2.0
		.10	1.7	0.9	4.6
		.20	2.7	5.9	4.5
	3 Hrs.	.10		3.2	
	6 Hrs.	.10		7.2	
B-2960	0	.10	0.6	2.9	
	6 Hrs.	.10		5.8	
B-3056	0	.10	6.1	7.1	
	6 Hrs.	.10		1.7	

* - For n values of X, where \bar{X} is the average value of the X's, the coefficient of variation is defined by:

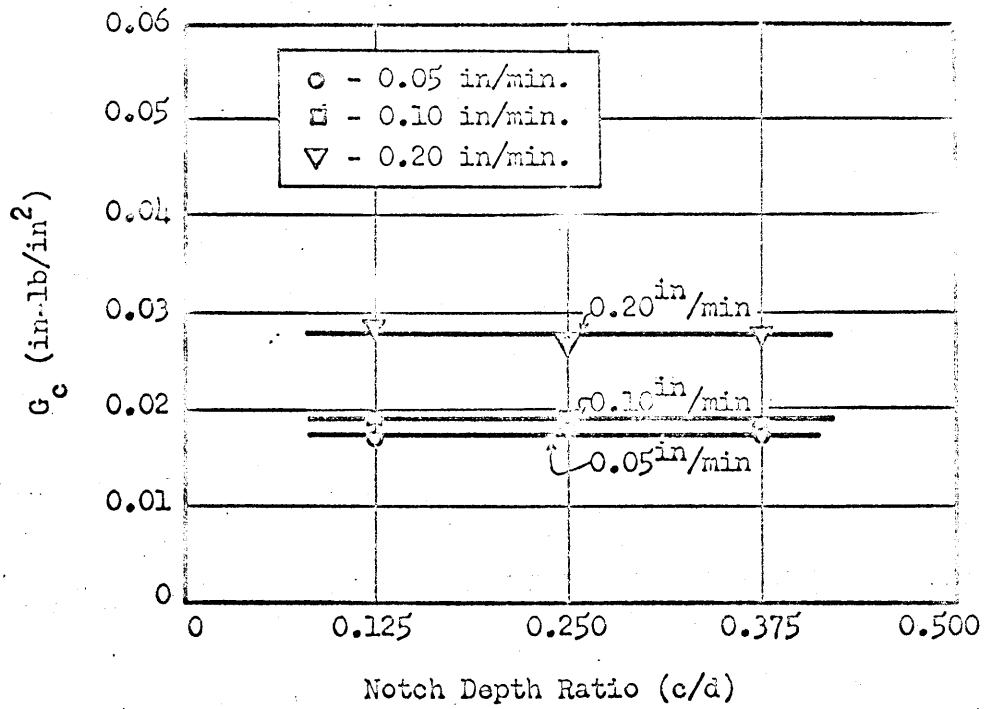


Figure 5 -- G_c versus c/d for the Unaged 60-70 Asphalt at +7°F.

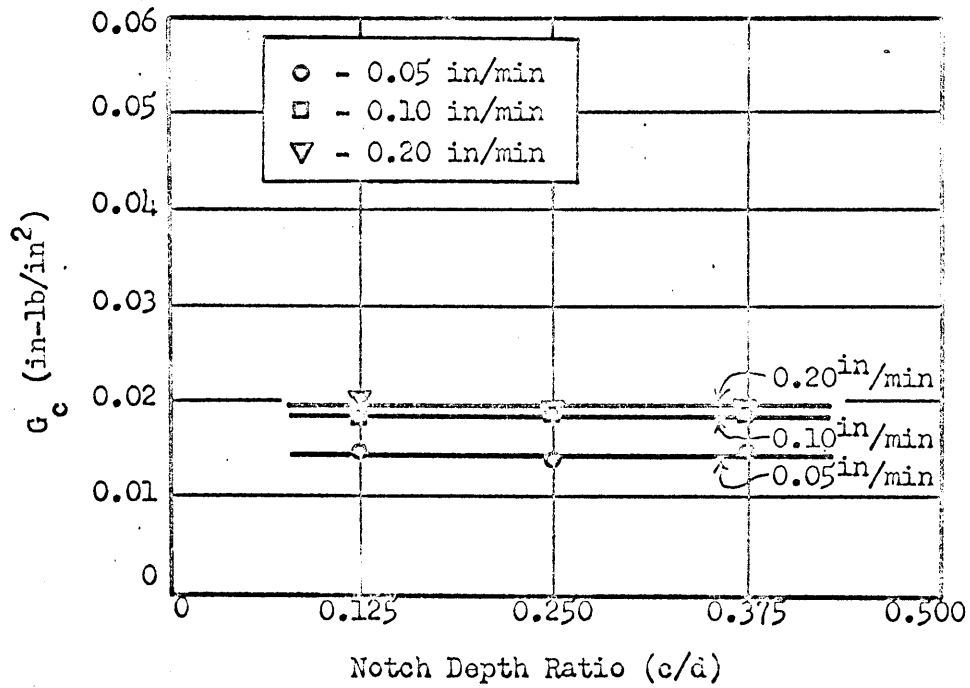


Figure 6 -- G_c versus c/d for the Unaged 60-70 Asphalt at 0°F.

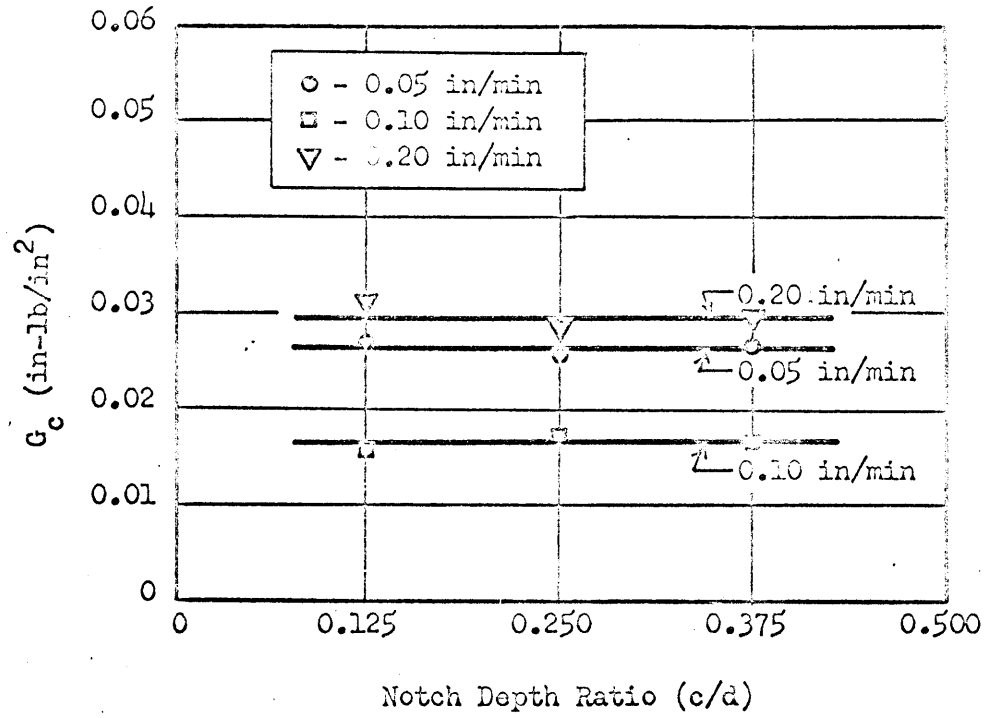


Figure 7 -- G_c versus c/d for the Unaged 60-70 Asphalt at -7°F .

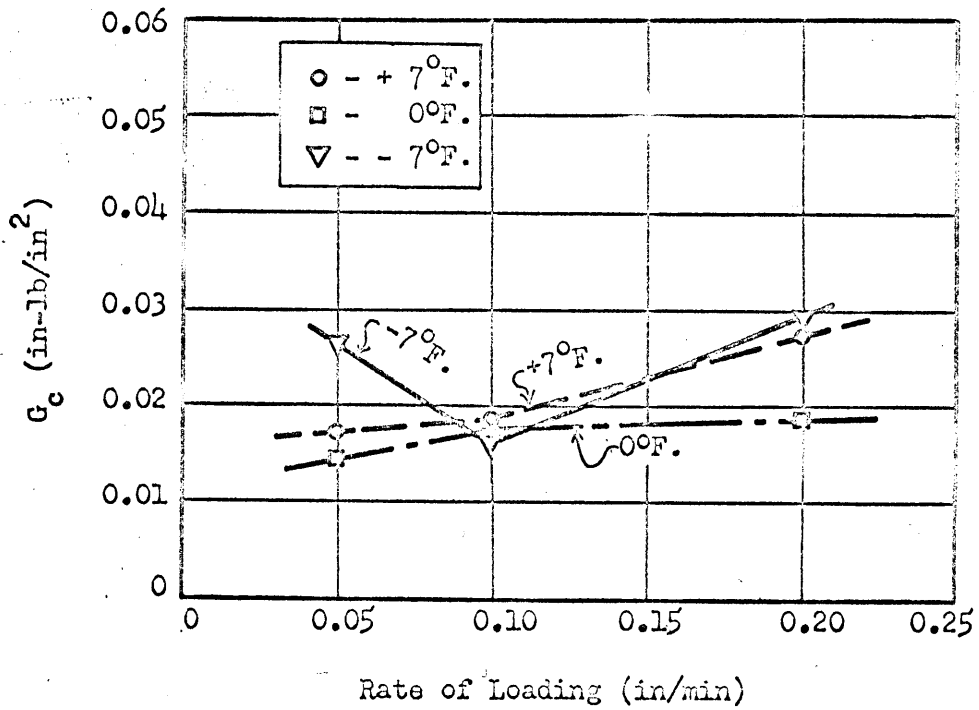


Figure 8 -- G_c versus the Rate of Loading for the Unaged 60-70 Asphalt

loading rates, and at three different test temperatures. The variations of G_c versus the rate of loading for different test temperatures are plotted in Figure 8. This figure indicates that the critical strain-energy release rate is dependent on the loading rate and varying with the temperature.

Effect of Temperature

The values of G_c for three different loading rates are plotted versus the notch depth ratio in Figures 9 through 11 with each figure showing the results at different test temperatures. These values are again for the 60-70 penetration grade asphalt in the unaged condition. In Figure 12, G_c is plotted versus the test temperature for three different loading rates. This figure indicates the dependency of the critical strain-energy release rate upon the temperature. This dependency varies with the loading rate.

Effect of Different Asphalts

In Figures 13 and 14, the values of G_c are plotted versus the notch depth ratio for two different unaged asphalts, the B-3056 and the B-2960 asphalts, respectively, at a rate of loading of 0.10 inches/minute. Under these conditions, these two asphalts exhibit similar behaviour to that of the 60-70 asphalt, Figure 10, which is increasing values of G_c from 0°F. to +7°F. The B-2960 asphalt is the most temperature sensitive of the three asphalts as is shown in Figure 15, where G_c is plotted versus the temperature for the three asphalts. The relative difference in the behaviours of the different asphalts at two temperatures is shown in this figure. The values of G_c for the 60-70 and the B-3056 asphalts are rela-

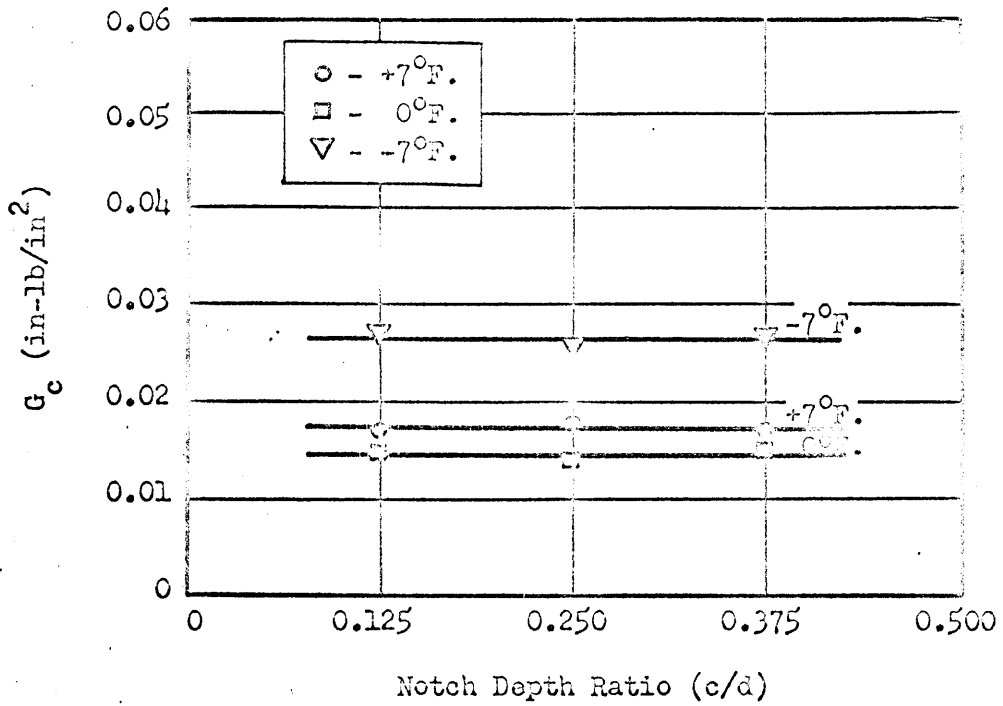


Figure 9 -- G_c versus c/d for the Unaged 60-70 Asphalt, Loaded at 0.05 inches/minute.

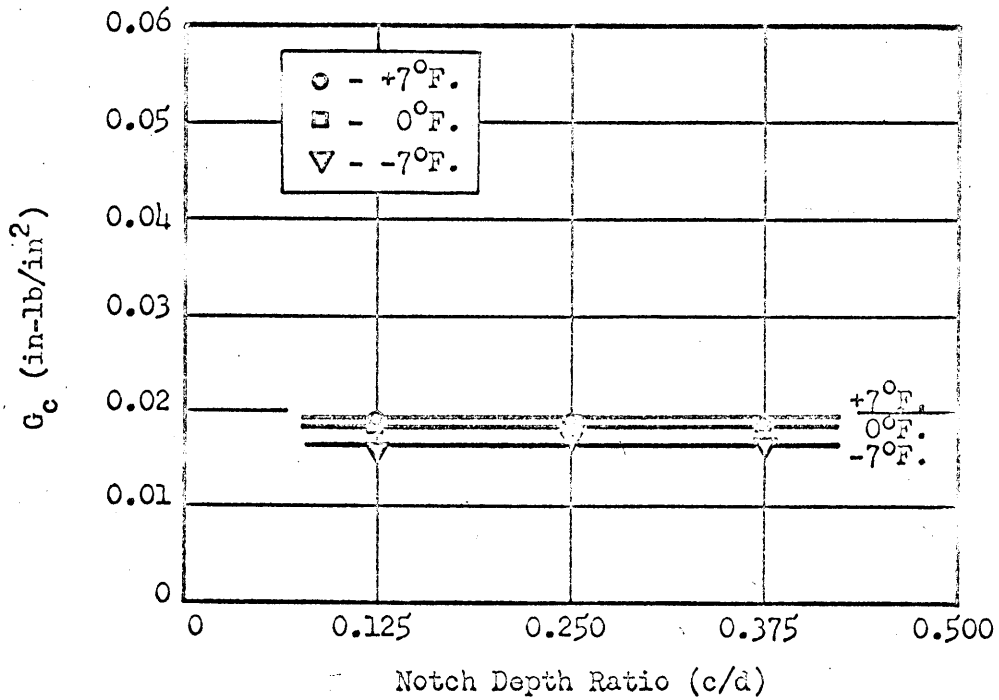


Figure 10 -- G_c versus c/d for the Unaged 60-70 Asphalt, Loaded at 0.10 inches/minute.

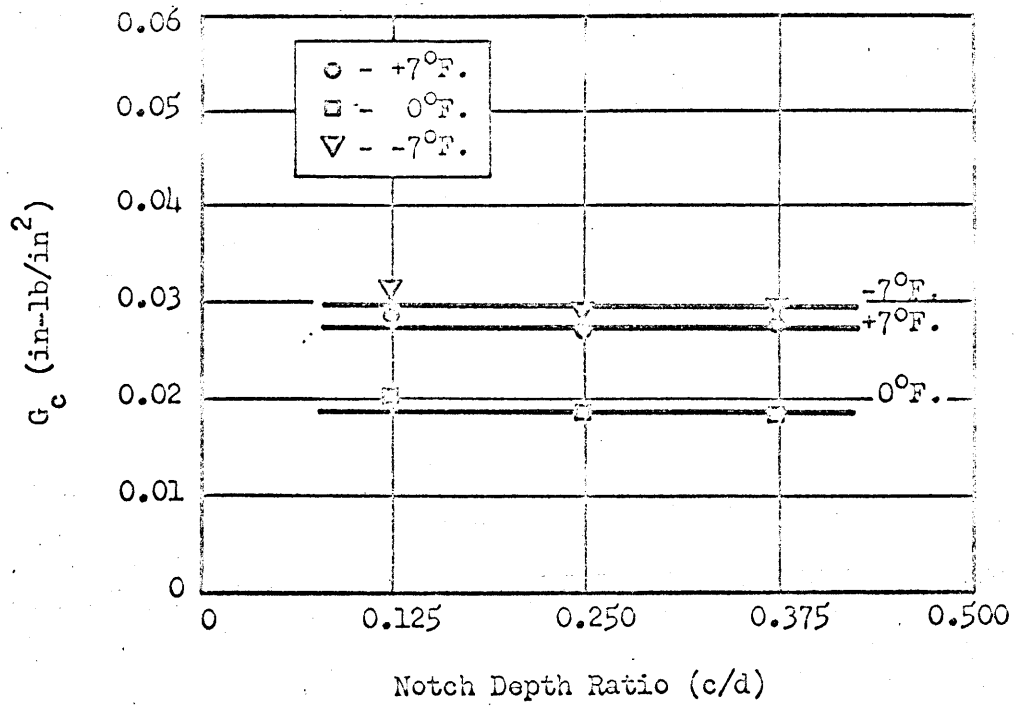


Figure 11 -- G_c versus c/d for the Unaged 60-70 Asphalt, Loaded at 0.20 inches/minute.

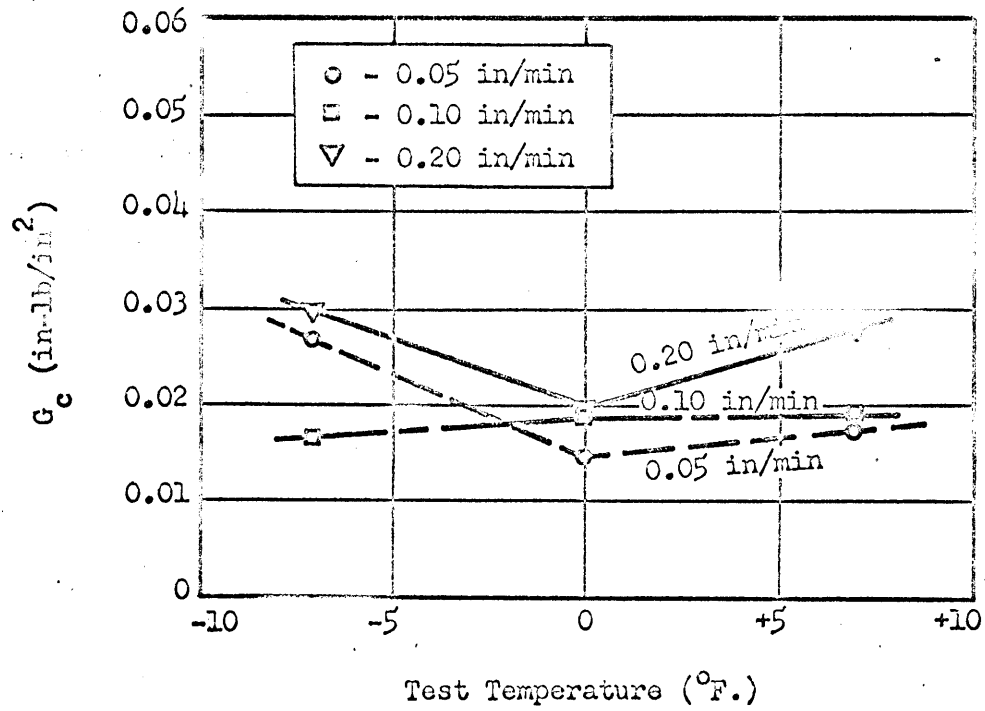


Figure 12 -- G_c versus the Test Temperature for the Unaged 60-70 Asphalt.

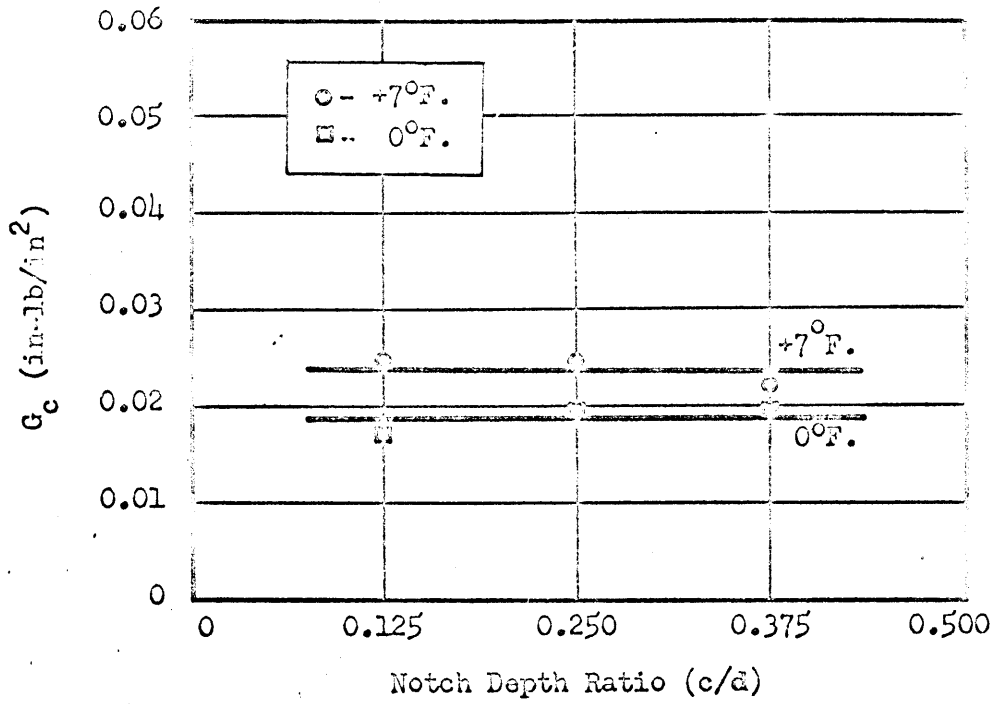


Figure 13 -- G_c versus c/d for the Unaged B-3056 Asphalt, Loaded at 0.10 inches/minute.

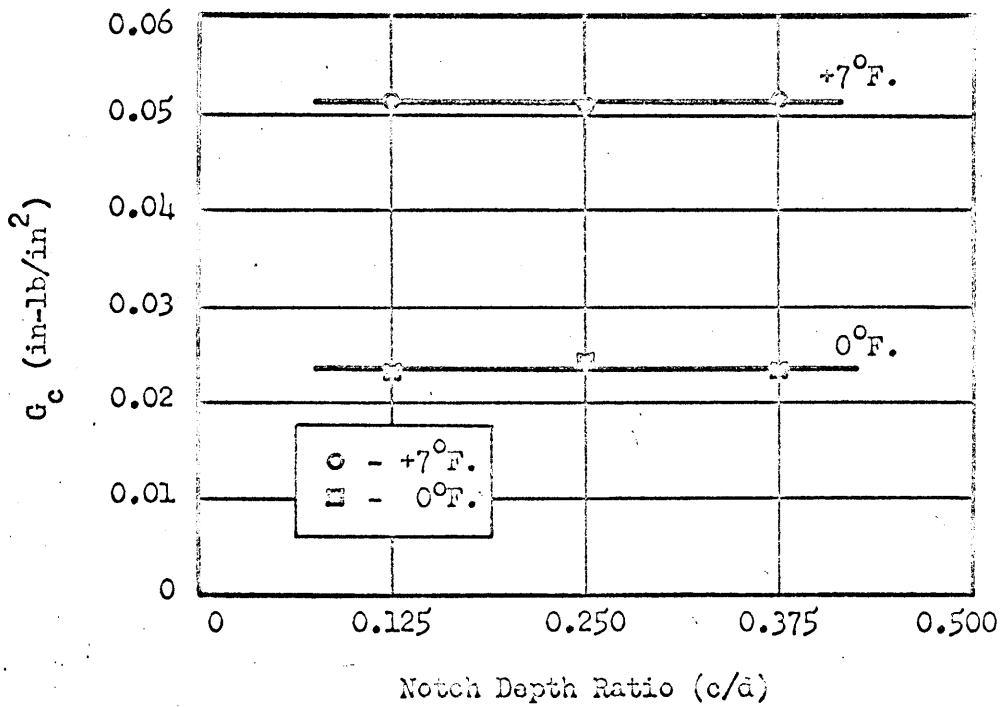


Figure 14 -- G_c versus c/d for the Unaged B-2960 Asphalt, Loaded at 0.10 inches/minute.

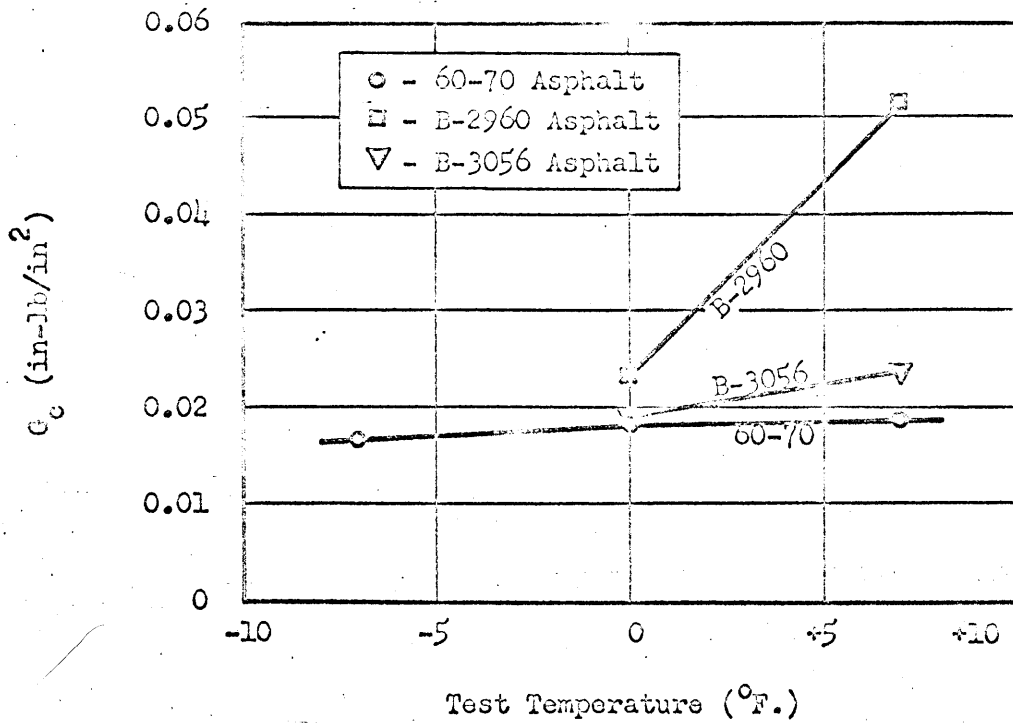


Figure 15 -- G_c versus the Test Temperature for the Unaged Asphalts, Loaded at 0.10 inches/minute.

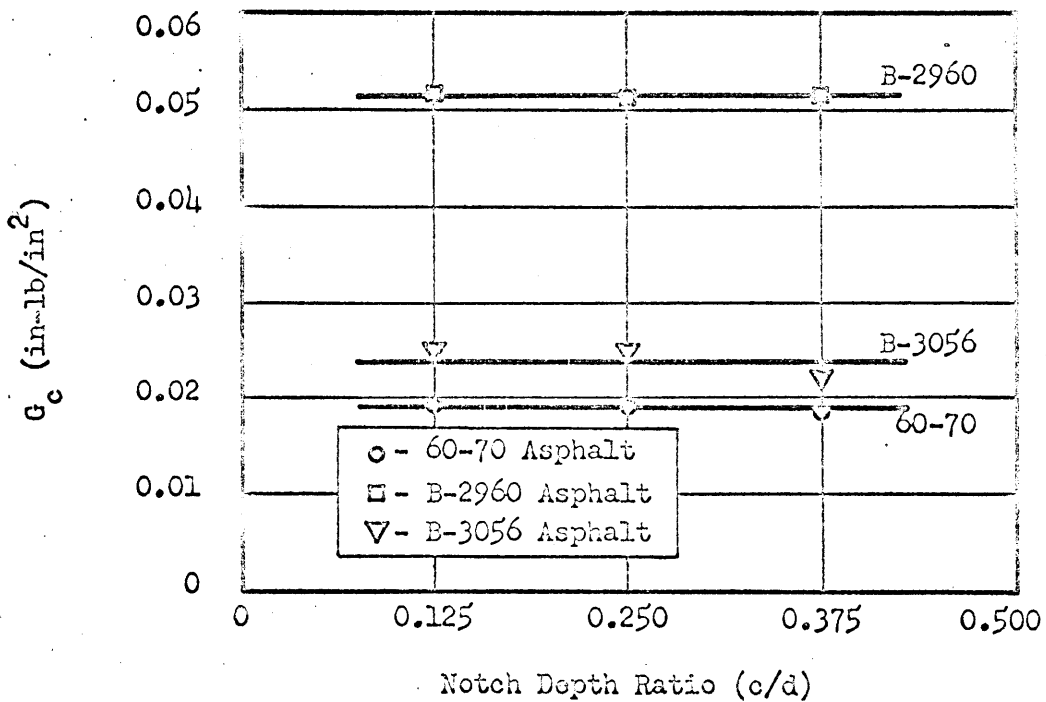


Figure 16 -- G_c versus c/d for the Unaged Asphalts, Loaded at 0.10 inches/minute, Tested at +7°F.

tively close at temperatures of 0°F . and $+7^{\circ}\text{F}$. with the 60-70 having slightly lower values of G_c at each temperature. The values of G_c for the B-2960 asphalt are considerably higher than the values for the other two asphalts, being more than twice as much at $+7^{\circ}\text{F}$. In Figures 16 and 17, G_c is plotted versus the notch depth ratio, for the unaged asphalts tested at 0.10 inches/minute, again showing the difference in the asphalts at different temperatures.

Effect of Aging

In Figure 18, the values of G_c are plotted versus the notch depth ratio for the three asphalts after six hours of aging at 375°F . This figure shows the same relative behaviour between asphalts as was present with no aging, Figure 17, i.e., the B-2960 asphalt and the 60-70 asphalt, have the highest and lowest values, respectively, of G_c . However, the behaviour of the individual asphalts varies considerably due to aging as can be seen in Figures 19 through 21 where G_c is plotted versus the notch depth ratio for each of the asphalts after different aging times. The variation of G_c versus the degree of aging for the three asphalts is shown in Figure 22. The two asphalts which show the most Newtonian behaviour, the 60-70 penetration and the B-2960 asphalts, both exhibit increasing values of G_c with aging while the other asphalt, the B-3056, shows decreasing values of G_c with aging. In fact, for the two asphalts which are the most Newtonian, the value of G_c approximately doubles from no aging to six hours aging while for the third asphalt, the B-3056, the value of G_c drops approximately twenty per cent.

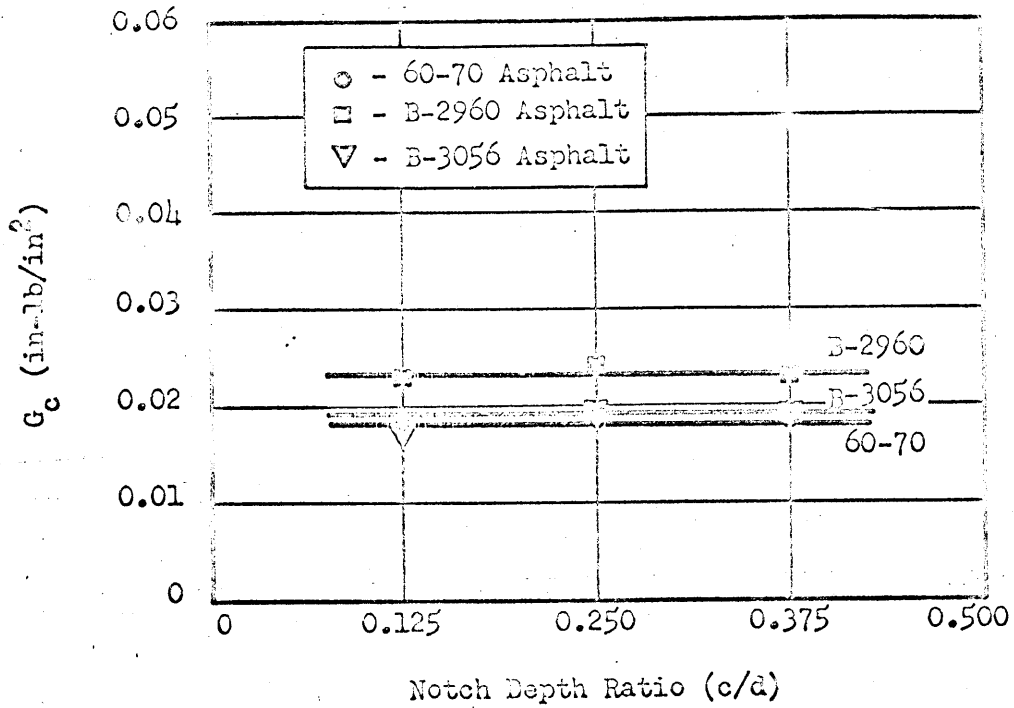


Figure 17 -- G_c versus c/d for the Unaged Asphalts, Loaded at 0.10 inches/minute, Tested at 0°F.

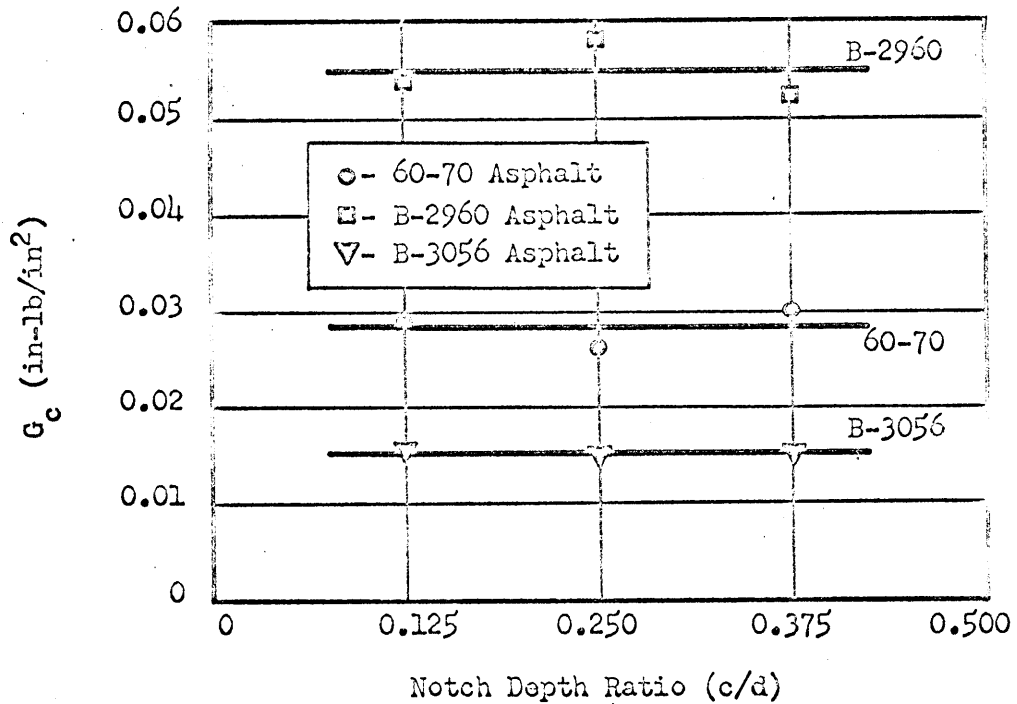


Figure 18 -- G_c versus c/d for the Asphalts Aged Six Hours at 375°F., Loaded at 0.10 inches/minute, and Tested at 0°F.

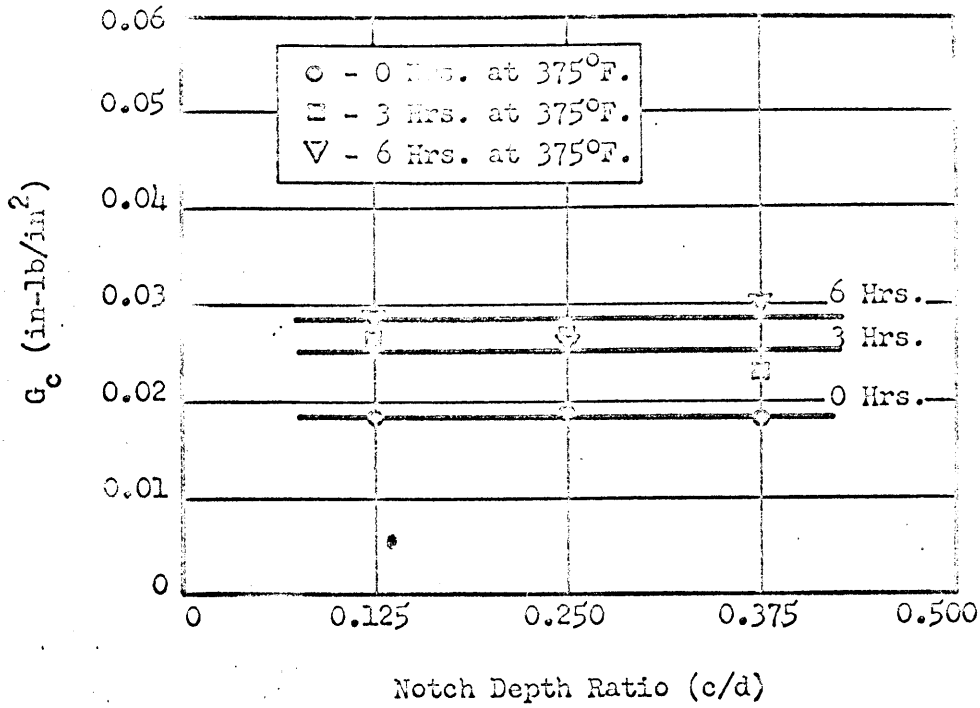


Figure 19 -- G_c versus c/d for the 60-70 Asphalt,
Loaded at 0.10 inches/minute,
Tested at 0°F.

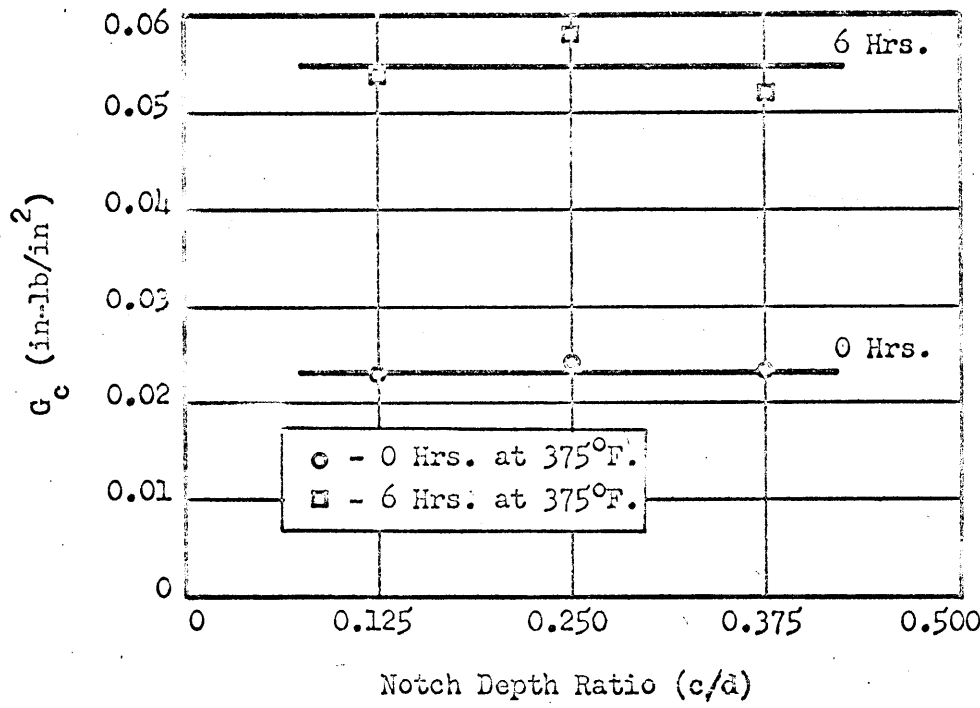


Figure 20 -- G_c versus c/d for the B-2960 Asphalt,
Loaded at 0.10 inches/minute,
Tested at 0°F.

CONCLUSIONS

In this investigation, tests on notched beams are used for the determination of the critical strain-energy release rate for three asphalts at various conditions. From the results of this study, the following conclusions are drawn:

1. At sufficiently low temperatures, the asphalts behave as brittle, amorphous materials and the Griffith theory of brittle fracture can be applied to study the fracture behaviour of asphalts.
2. The critical strain-energy release rate can be calculated for asphalts and its value is independent of the geometry of the specimen. The value of the critical strain-energy release rate is influenced by the rate of loading, the test temperature, and the type of asphalt.
3. The degree of aging has a significant influence on the calculated values of the critical strain-energy release rate.

The results of this study also indicate the need for, and the possibilities of, further investigation in the following areas:

1. The study should be extended to include a wider range of temperatures and greater degrees of aging.
2. In order to establish specifications, further work must be done over a wider range of temperatures, more degrees of aging, and inclusion of mineral fillers in the asphalt.

REFERENCES

1. Vallerga, B. A., "On Asphalt Pavement Performance," Proceedings, Association of Asphalt Paving Technologists, Volume 24, 1955.
2. Finn, F. N., "Factors Involved in the Design of Asphalt Pavement Surfaces," Highway Research Board Report HR 1-8, March 1966.
3. Griffith, A. A., "The Phenomena of Rupture and Flow in Solids," Philosophical Transactions, Royal Society of London, Series A, Volume 221, 1920.
4. Inglis, C. E., "Stresses in a Plate Due to the Presence of Cracks and Sharp Corners," Transactions, Institute of Naval Architects, Volume 55, 1913.
5. Griffith, A. A., "The Theory of Rupture," First International Congress of Applied Mechanics, Delft, 1924.
6. Orowan, E., "Fracture and Strength of Solids," Reports on Progress in Physics, Volume 12, 1949.
7. Irwin, G. R., "Fracture Dynamics," Fracturing of Metals, American Society of Metals, Cleveland, Ohio, 1948.
8. Orowan, E., "Fundamentals of Brittle Behaviour in Metals," Fatigue and Fracture of Metals, (MIT Symposium, June, 1950), John Wiley and Sons, Inc., New York, 1950.
9. Irwin, G. R., "Relation of Stresses Near a Crack to the Crack Extension Force," Proceedings, Ninth International Congress of Applied Mechanics, Paper No. 101 (11), Brussels, 1956.
10. Irwin, G. R., "Fracture Mechanics," First Symposium on Naval Structural Mechanics, Stanford University, August, 1958.
11. Kaplan, M. F., "Crack Propagation and the Fracture of Concrete," Proceedings, Journal of the American Concrete Institute, Volume 58, 1961.
12. Moavenzadeh, F. and R. R. Stander, Jr., "Effect of Aging of Asphalt on its Rheological Properties," Journal of Materials, Volume 1, No. 1, March, 1966.

A P P E N D I C E S

DEFINITIONS OF SYMBOLS

- c = notch depth
- d = over-all depth of beam
- h = net depth of beam at notch = d-c
- l = span length
- n = constant
- y = deflection
- A = constant
- E = modulus of elasticity
- G = strain-energy release rate
- G_c = critical strain-energy release rate
- I = moment of inertia
- P = applied load
- U = release of strain-energy due to formation of the crack
- W = work done in the course of crack formation
- γ = surface energy of the material per unit area
- γ_p = surface work of the material per unit area
- $\dot{\gamma}$ = shear rate
- μ = Poisson's ratio
- ρ = radius of the notch at the root of the notch
- σ = stress
- σ_m = maximum stress at the root of the notch
- σ_n = nominal stress at the root of the notch
- τ = shear stress

LIST OF FIGURES

<u>FIGURE</u>	<u>PAGE</u>
1 . Values of $f(c/d)$ versus the Notch Depth Ratio	13
2 . Shear Rate versus Shear Stress at 25°C.	17
3 . Notch Geometry and Method of Loading of the Beams	18
4 . Schematic Load-Deflection Diagram	20
5 . G_c versus c/d for the Unaged 60-70 Asphalt at +7°F.	26
6 . G_c versus c/d for the Unaged 60-70 Asphalt at 0°F.. . . .	26
7 . G_c versus c/d for the Unaged 60-70 Asphalt at -7°F.	27
8 . G_c versus the Rate of Loading for the Unaged 60-70 Asphalt.	27
9 . G_c versus c/d for the Unaged 60-70 Asphalt, Loaded at 0.05 inches/minute.	29
10 . G_c versus c/d for the Unaged 60-70 Asphalt, Loaded at 0.10 inches/minute.	29
11 . G_c versus c/d for the Unaged 60-70 Asphalt, Loaded at 0.20 inches/minute.	30
12 . G_c versus the Test Temperature for the Unaged 60-70 Asphalt	30
13 . G_c versus c/d for the Unaged B-3056 Asphalt, Loaded at 0.10 inches/minute.	31
14 . G_c versus c/d for the Unaged B-2960 Asphalt, Loaded at 0.10 inches/minute.	31
15 . G_c versus the Test Temperature for the Unaged Asphalts, Loaded at 0.10 inches/minute	32
16 . G_c versus c/d for the Unaged Asphalts, Loaded at 0.10 inches/minute, Tested at +7°F.. . . .	32
17 . G_c versus c/d for the Unaged Asphalts, Loaded at 0.10 inches/minute, Tested at 0°F.	34
18 . G_c versus c/d for the Asphalts Aged Six Hours at 375°F., Loaded at 0.10 inches/minute, and Tested at 0°F.	34

LIST OF FIGURES (Continued)

<u>FIGURE</u>		<u>PAGE</u>
19	. G_c versus c/d for the 60-70 Asphalt, Loaded at 0.10 inches/minute, Tested at 0°F.	35
20	. G_c versus c/d for the B-2960 Asphalt, Loaded at 0.10 inches/minute, Tested at 0°F.	35
21	. G_c versus c/d for the B-3056 Asphalt, Loaded at 0.10 inches/minute, Tested at 0°F.	36
22	. G_c versus Aging Time at 375°F. for the Asphalts Loaded at 0.10 inches/minute, Tested at 0°F.	36

LIST OF TABLES

<u>TABLE</u>	<u>PAGE</u>
1 . Test Variables Used in this Study	14
2 . Results of Conventional Tests on Asphalts Used in this Study	16
3 . Calculated Moduli of Elasticity	22
4 . Values of $f(c/d)$ Used	22
5 . Values of the Critical Strain-Energy Release Rate for Different Notch Depth Ratios	23
6 . Average Values of the Critical Strain-Energy Release Rate	24
7 . Values of the Coefficient of Variation.	25

LIST OF TABLES

<u>TABLE</u>	<u>PAGE</u>
1 . Test Variables Used in this Study	14
2 . Results of Conventional Tests on Asphalts Used in this Study	16
3 . Calculated Moduli of Elasticity	22
4 . Values of $f(c/d)$ Used	22
5 . Values of the Critical Strain-Energy Release Rate for Different Notch Depth Ratios	23
6 . Average Values of the Critical Strain-Energy Release Rate	24
7 . Values of the Coefficient of Variation.	25